

# Constraining Neutron-Star Matter with Microscopic and Macroscopic Collisions

Sabrina Huth, Peter T. H. Pang, Ingo Tews, Tim Dietrich, [Arnaud Le Fèvre](#), Achim Schwenk, Wolfgang Trautmann, Kshitij Agarwal, Mattia Bulla, Michael W. Coughlin, and Chris Van Den Broeck - [arXiv:2107.06229 \(2021\)\[nucl-th\]](#)

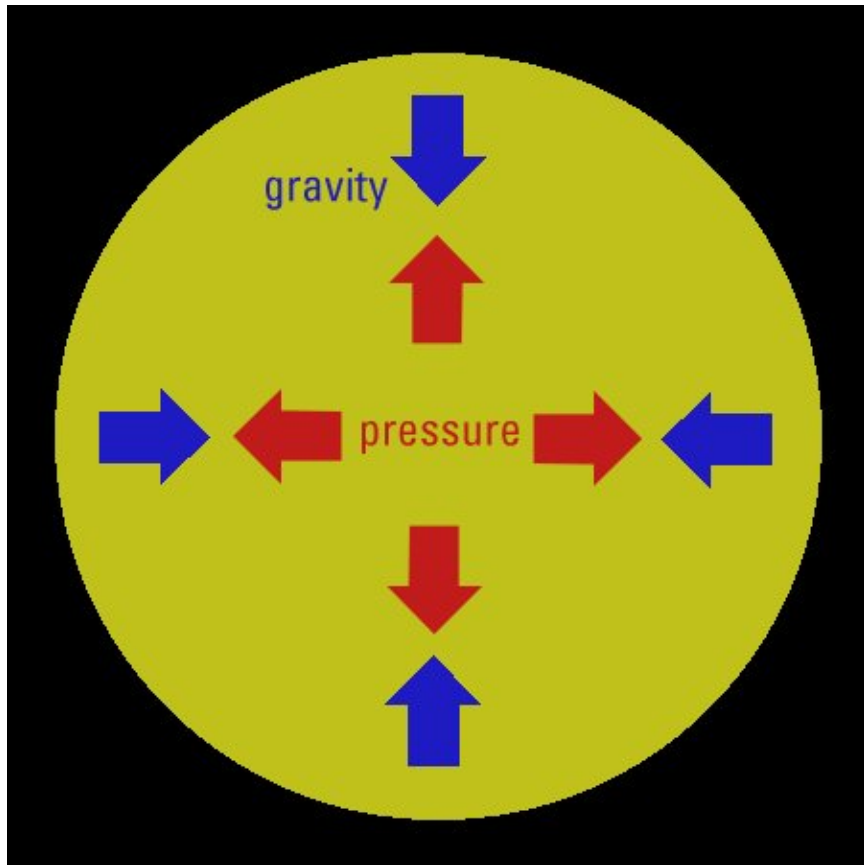
# Constraining Neutron-Star Matter with Microscopic and Macroscopic Collisions

Sabrina Huth, Peter T. H. Pang, Ingo Tews, Tim Dietrich, Arnaud Le Fèvre, Achim Schwenk, Wolfgang Trautmann, Kshitij Agarwal, Mattia Bulla, Michael W. Coughlin, and Chris Van Den Broeck - [arXiv:2107.06229 \(2021\)\[nucl-th\]](https://arxiv.org/abs/2107.06229)

- Nuclear theory input (chiral effective field theory for nuclear forces)
- Multi-messenger astrophysics information
- Data from HIC experiments
- Final constraints on the pressure and the radius of neutron stars
- HIC input perspectives: Towards larger densities and improved accuracy...

# Why are stars stable?

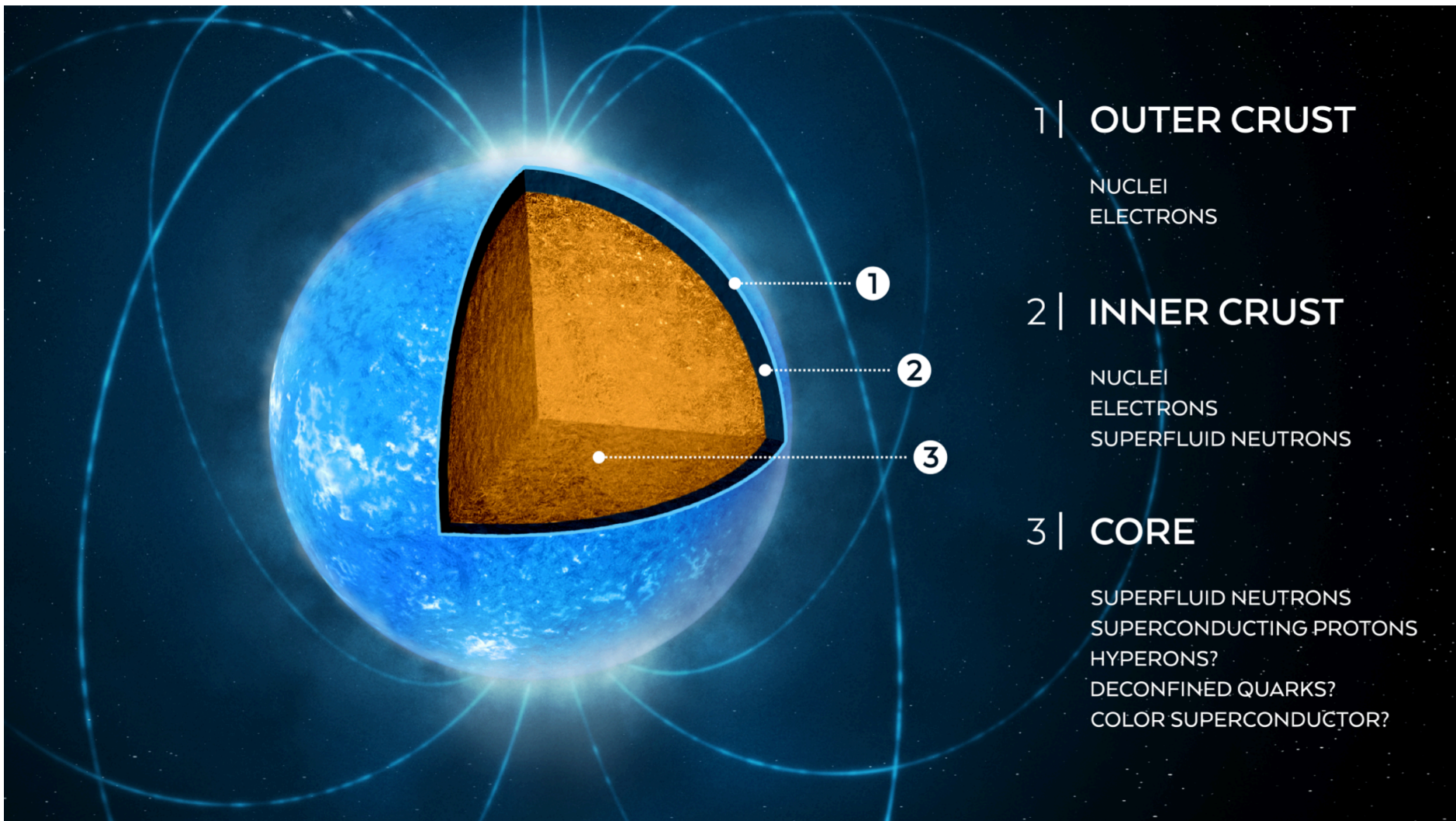
- Due to their mass, stars would undergo gravitational collapse
- Stabilised by the pressure of matter they consist of:  
equation of state → hydrostatic equilibrium



For neutrons:  
pressure of Fermi gas  
plus strong interactions

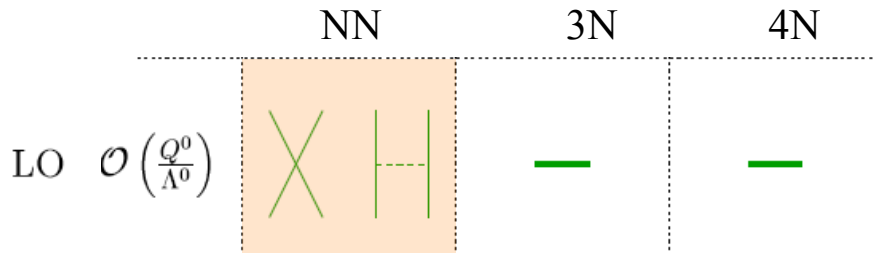
# Extreme matter in neutron stars

Governed by the same strong interactions



# Chiral effective field theory for nuclear forces

Systematic momentum expansion of nuclear forces (power counting) in low momenta ( $Q/\Lambda$ )



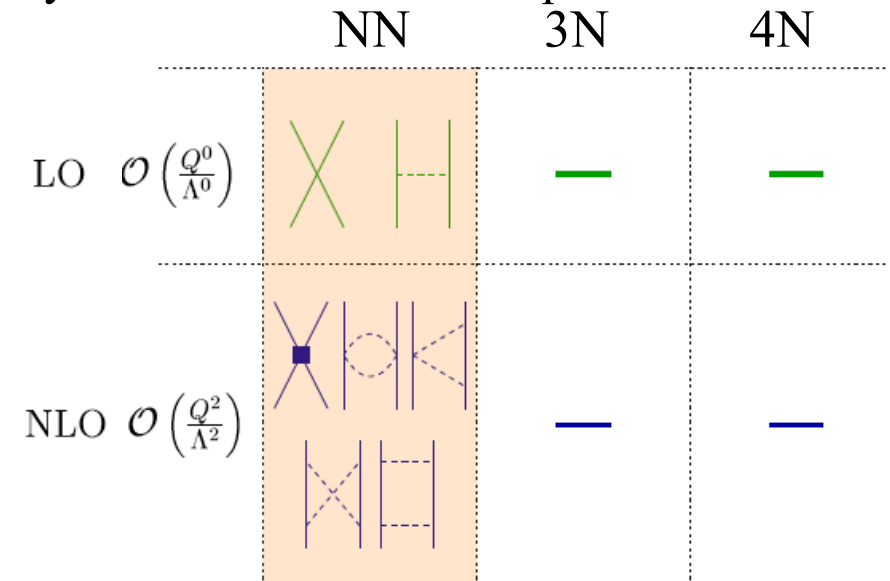
- Based on symmetries of strong interaction (QCD) between nucleons
- Long-range interactions governed by pion exchanges
- Expansion enables estimates of theoretical uncertainties
- Use of quantum Monte Carlo methods, which are among the most precise many-body methods to solve the nuclear many-body problem



Weinberg (1990,91)

# Chiral effective field theory for nuclear forces

Systematic momentum expansion of nuclear forces (power counting) in low momenta ( $Q/\Lambda$ )



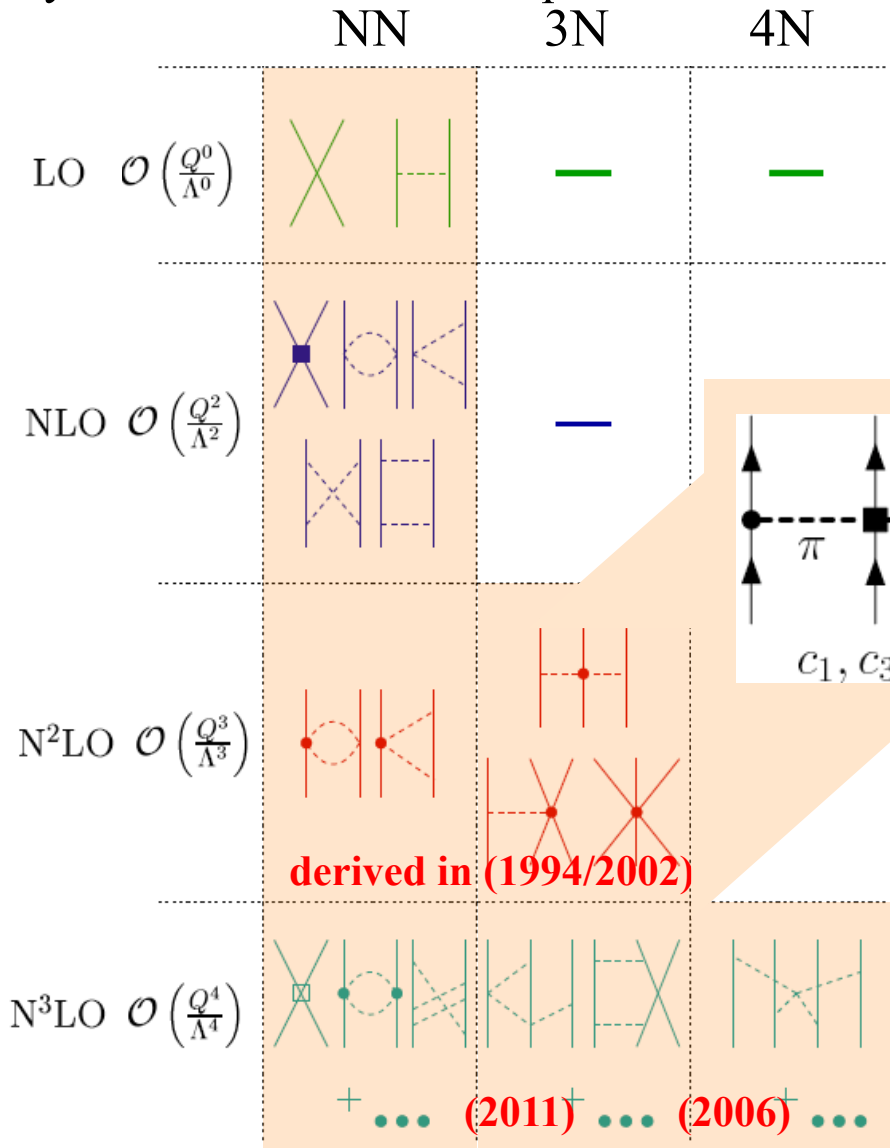
- Based on symmetries of strong interaction (QCD) between nucleons
- Long-range interactions governed by pion exchanges
- Expansion enables estimates of theoretical uncertainties
- Use of quantum Monte Carlo methods, which are among the most precise many-body methods to solve the nuclear many-body problem



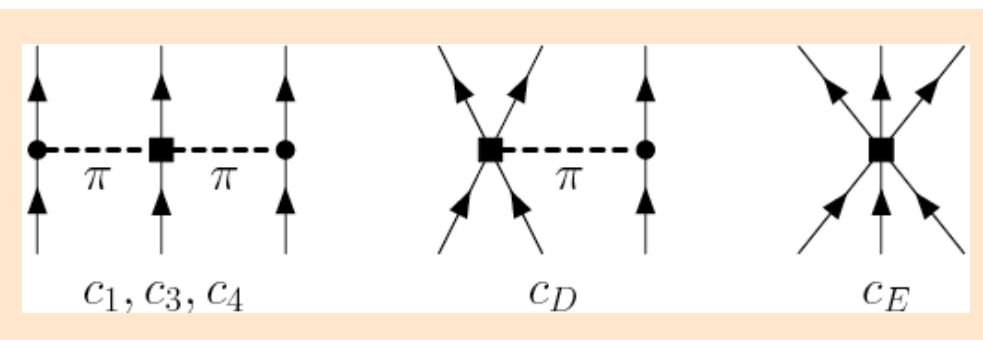
Weinberg (1990,91)

# Chiral effective field theory for nuclear forces

Systematic momentum expansion of nuclear forces (power counting) in low momenta ( $Q/\Lambda$ )



powerful approach for  
many-body interactions



only 2 new couplings at  $N^2LO$   
all 3- and 4-neutron forces  
predicted to  $N^3LO$

Weinberg, van Kolck (1992-1994), Kaplan,  
Savage, Wise, Bernard, Epelbaum, Kaiser, Meissner,...

# Chiral EFT calculations of neutron matter

IOP Publishing

J. Phys. G: Nucl. Part. Phys. **42** (2015) 034028 (20pp)

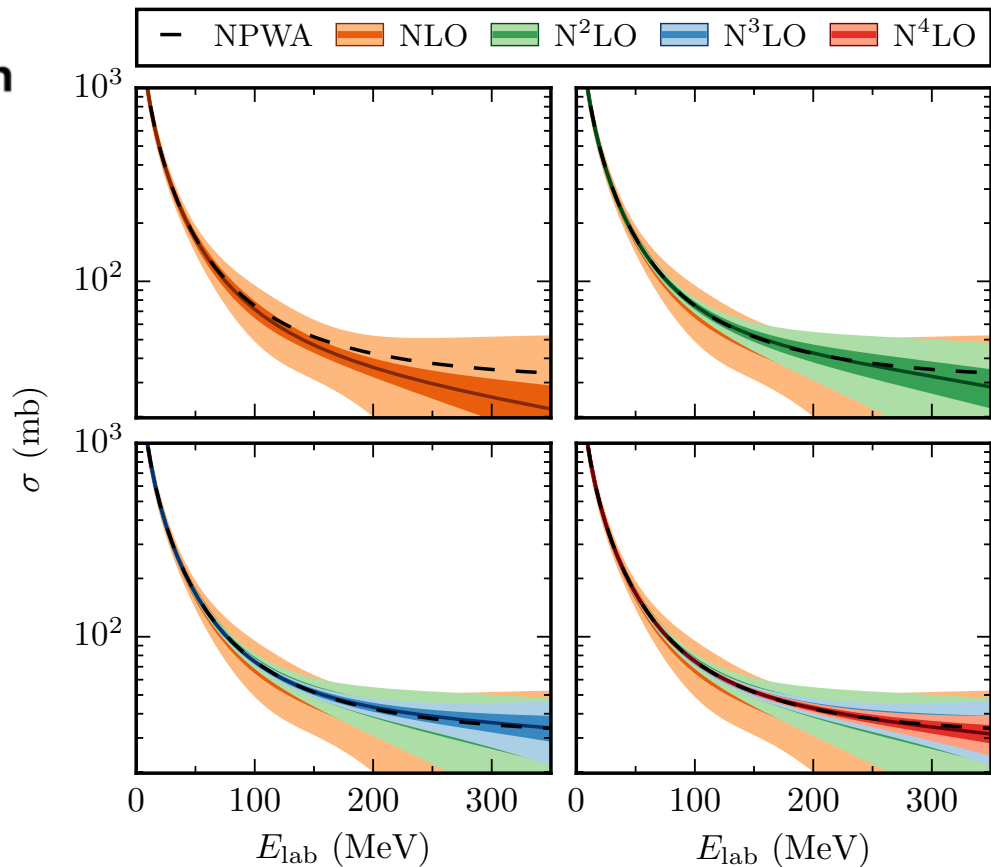
Journal of Physics G: Nuclear and Particle Physics

doi:10.1088/0954-3899/42/3/034028

Bayesian uncertainty estimates  
and model checking

## A recipe for EFT uncertainty quantification in nuclear physics

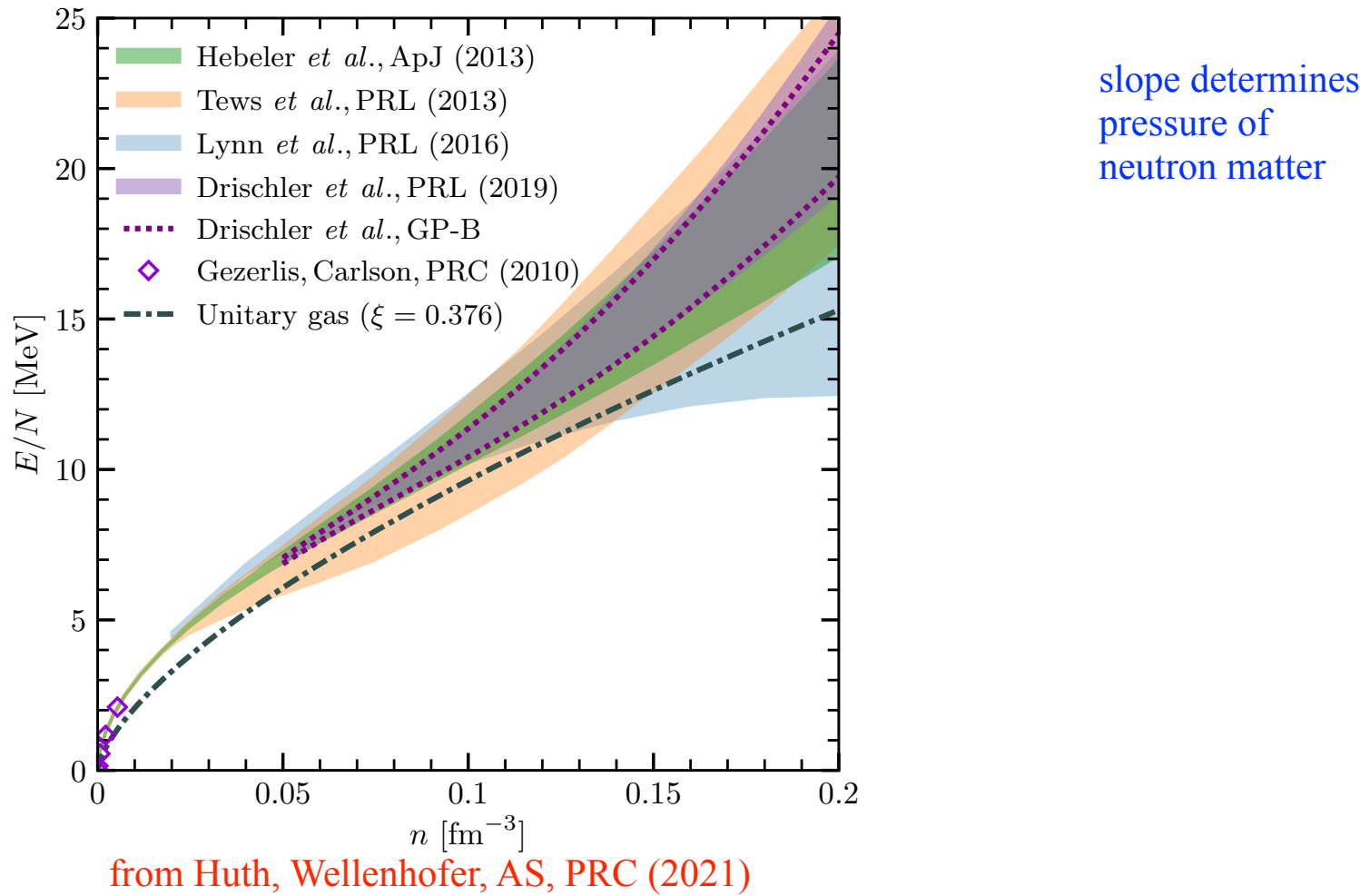
R J Furnstahl<sup>1</sup>, D R Phillips<sup>2</sup> and S Wesolowski<sup>1</sup>



Furnstahl, Phillips, Klos, Wesolowski, Melendez (2015-)

# Chiral EFT calculations of neutron matter

Good agreement up to saturation density for neutron matter  
nonlocal/local interaction and different calculations (MBPT, QMC, SCGF, CC)



# Chiral EFT calculations of neutron matter

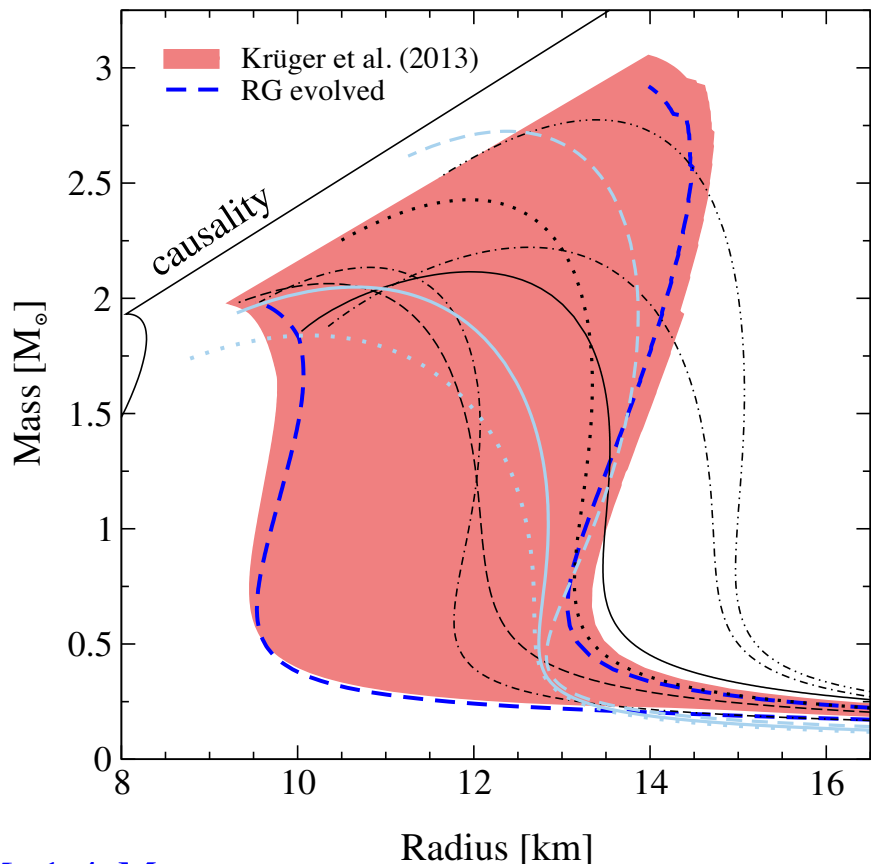
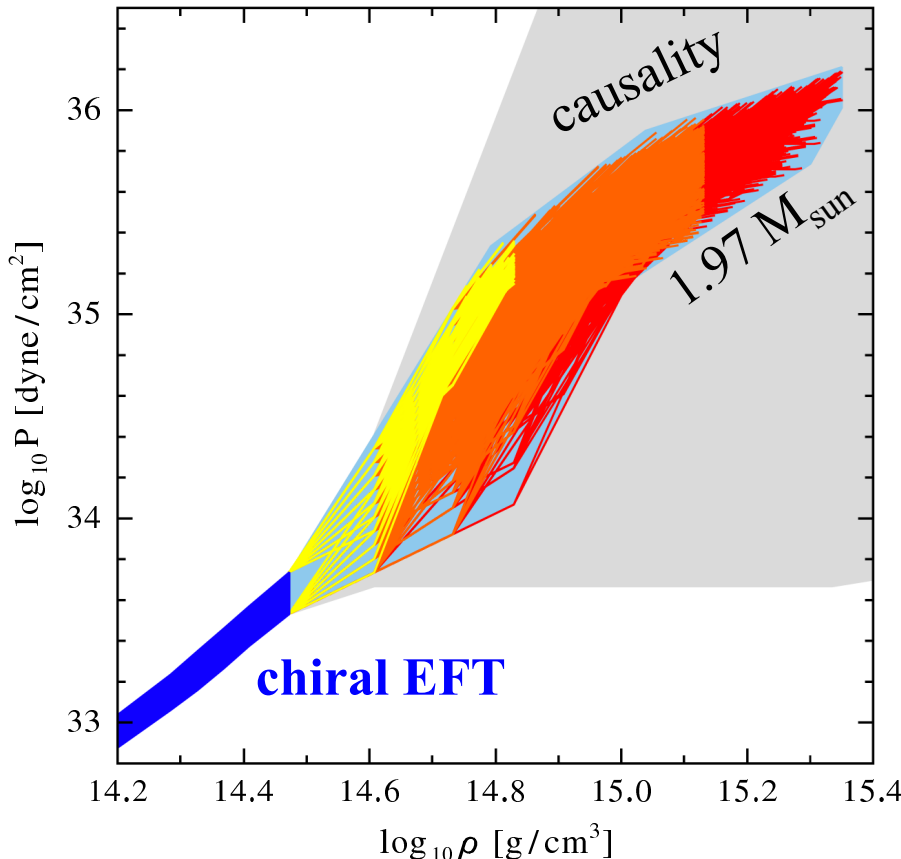
How is built the prior of the Bayesian analysis (quasi-Monte-Carlo results):

1. Generate a set of **15,000 EOSs** that are constrained by nuclear theory calculations at low densities (local chiral EFT interactions) → span the theoretical uncertainty range of the chiral EFT calculation.
2. Based on **local chiral 2- and 3-nucleon interactions**.
3. **Breakdown** scale of the chiral EFT expansion  $\sim 500\text{-}600 \text{ MeV}/c$ .  
⇒ constrain our EOS set using chiral EFT input only up to  $1.5\rho_0$  (corresponding to Fermi momenta of  $\sim 400 \text{ MeV}/c$ )
4. But a variation within  $1\text{-}2 \rho_0$  shows no substantial impact on our final results for neutron-star radii.
5. Extend each EOS above  $1.5\rho_0$  using an extrapolation in the speed of sound ( $c_s$ ) in neutron-star matter, with constraints of causality ( $c_s \leq c$ ) and stability of neutron-star matter ( $c_s \geq 0$ ).
6. Allow EOSs implying  $M_{NS} \geq 1.9M_\odot$ , to remove EOSs to support combined observations of heavy pulsars.
7. The EOS prior is then used to analyse astrophysical observations and HIC experiments.

# Impact on neutron stars

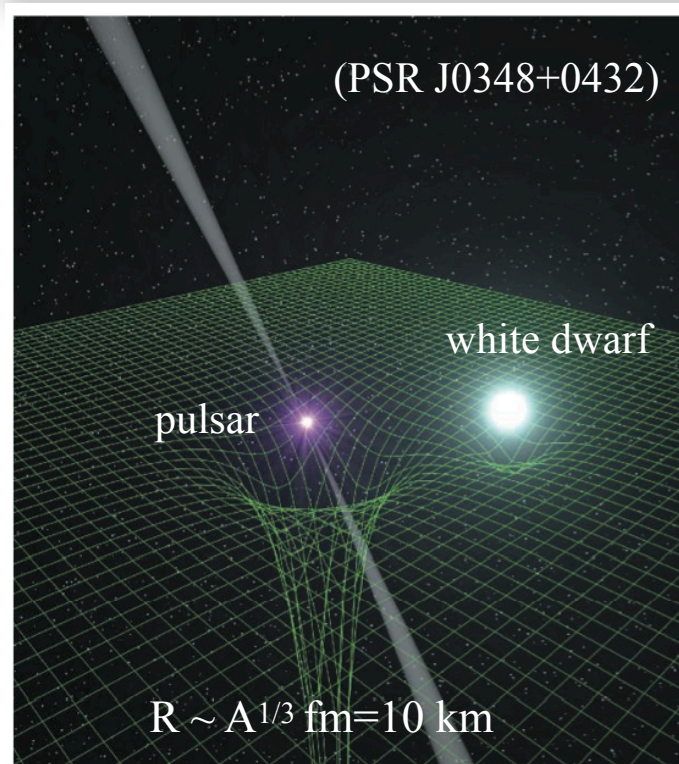
Hebeler et al., PRL (2010), ApJ (2013)

- Constrain high-density EOS by causality, require to support  $2 M_{\odot}$  star

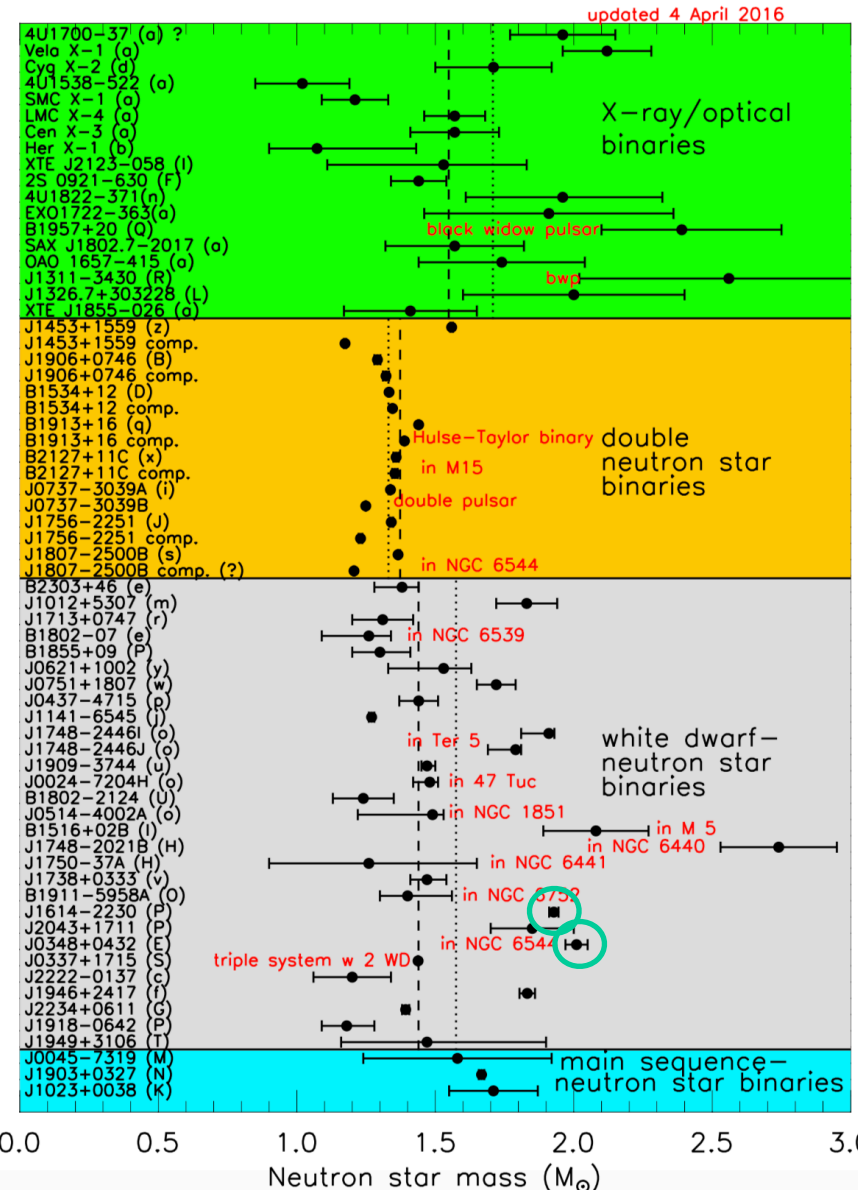


- Predicts neutron star radius:  $9.7 - 13.9$  km for  $M=1.4 M_{\odot}$   
1.8 - 4.4  $\rho_0$  modest central densities
- Speed of sound needs to exceed  $\sim 0.65c$  to get  $2 M_{\odot}$  stars Greif et al., ApJ (2020)

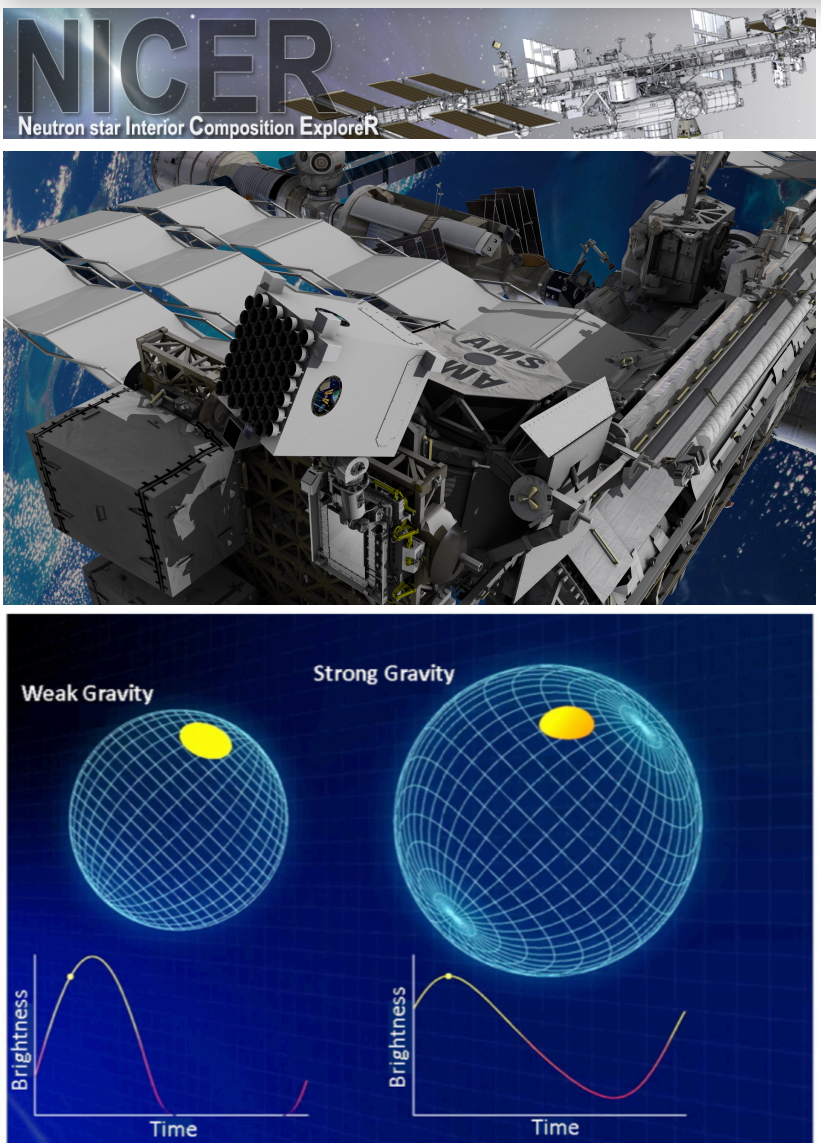
# Multi-messenger astrophysics information: Neutron star masses



from  
Jim Lattimer



# NICER results

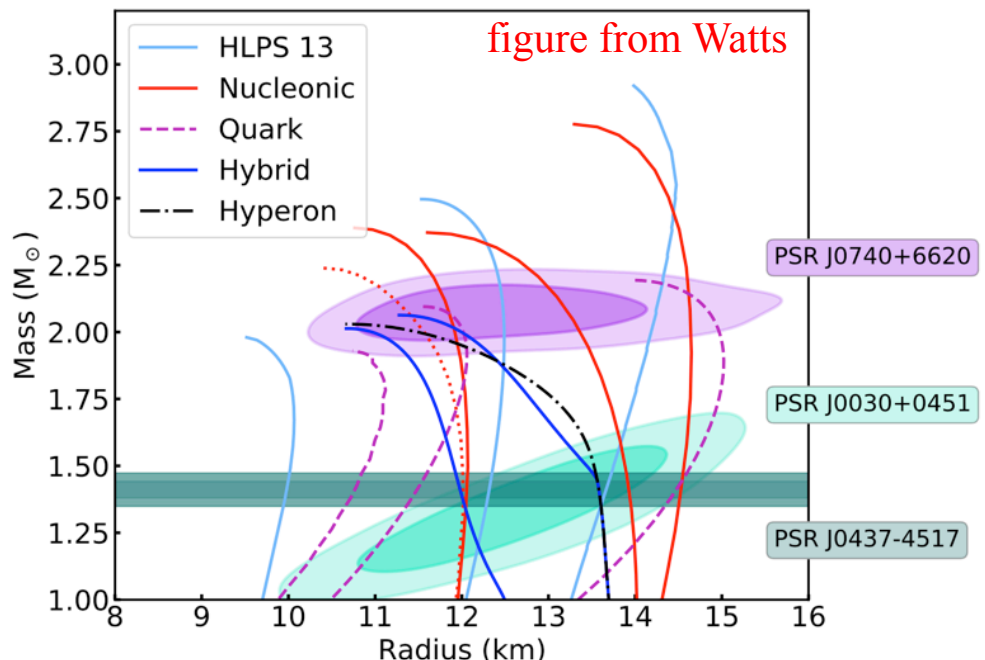
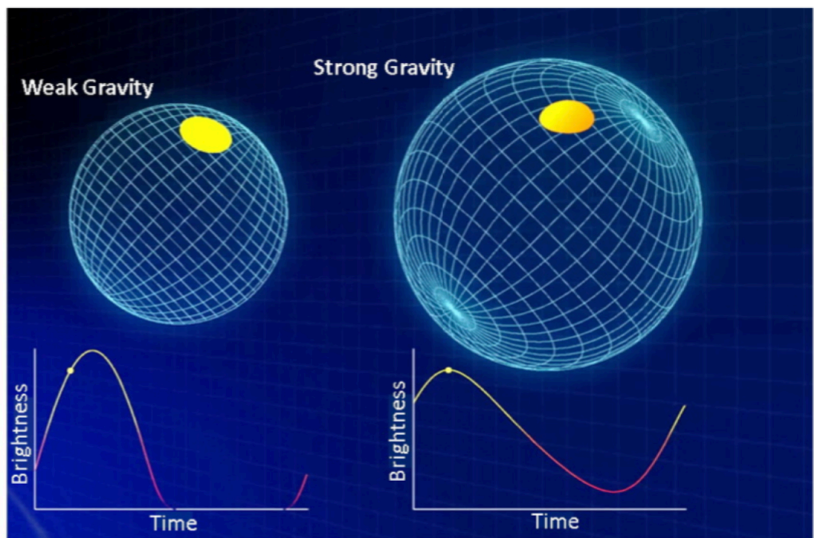


Neutron star radius from pulse profile modelling

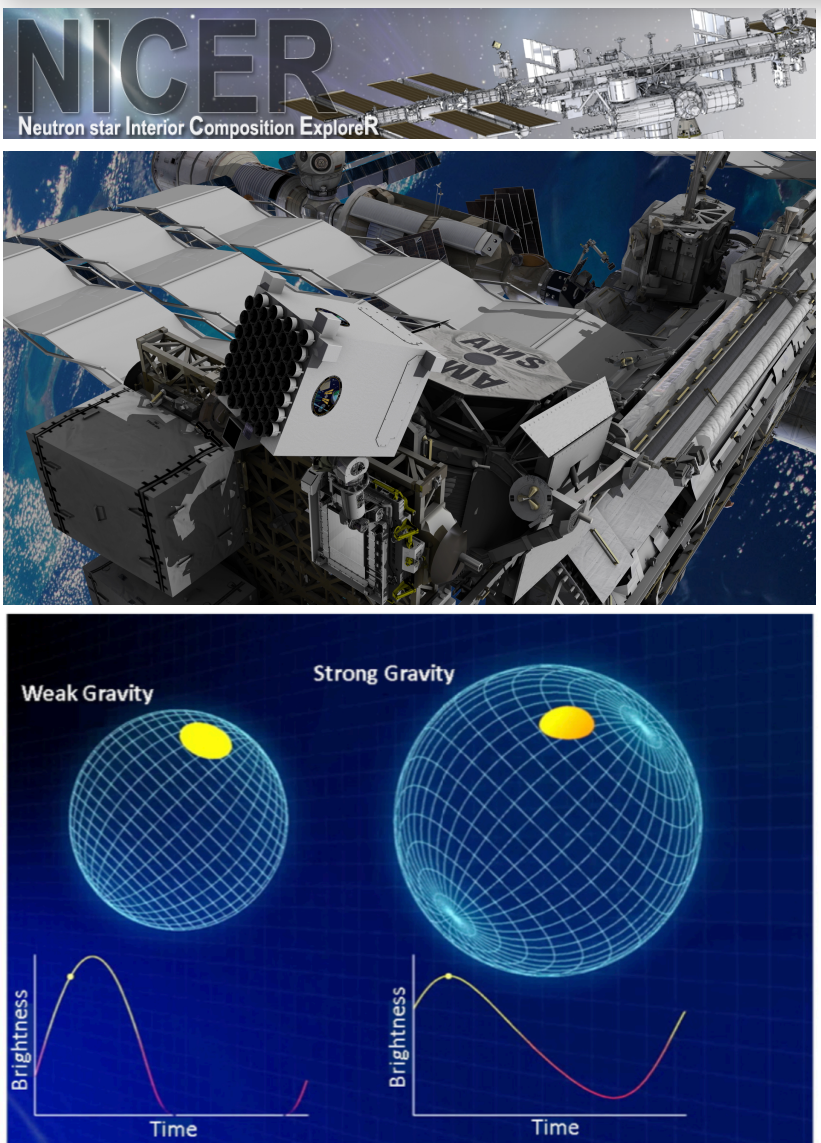
J0030 and J0740

here: Amsterdam analysis  
Riley et al., ApJL (2019), (2021)

similar results from Illinois-Maryland analysis  
Miller et al., ApJL (2019), (2021)



# NICER results

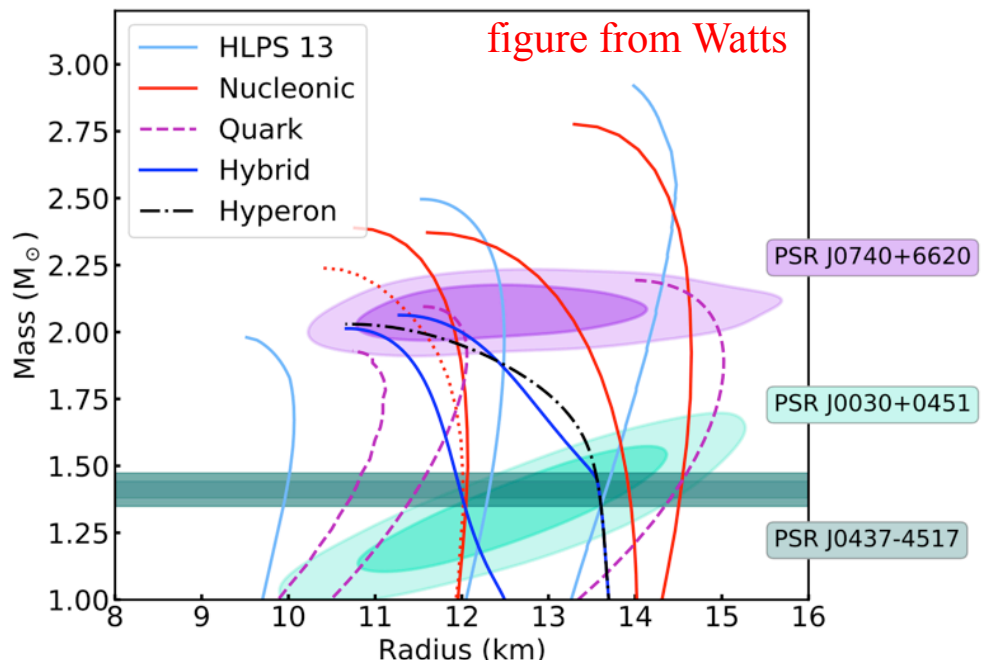
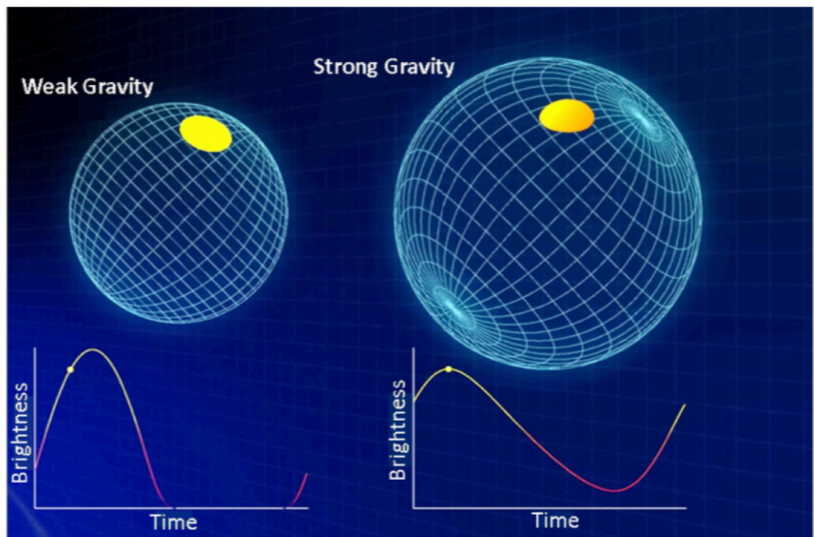


Neutron star radius from pulse profile modelling

J0030 and J0740

here: Amsterdam analysis  
Riley et al., ApJL (2019), (2021)

similar results from Illinois-Maryland analysis  
Miller et al., ApJL (2019), (2021)



# Multi-messenger astrophysics information

1. Mass measurements of the massive neutron stars PSR J0348+4042 and PSR J1614-2230  
→ lower bound on the NS maximum mass

2. Binary neutron-star collision GW170817  
in which a black hole was presumably formed after the coalescence maximum mass of neutron stars  
→ upper bound on the maximum mass.

3. X-ray pulse-profile modelling of PSR J0030+0451 and PSR J0740+6620 using data from NICER and the X-ray Multi-Mirror Mission (XMM-Newton) are incorporated.
4. Bayesian inference techniques to analyse GW information from the 2 neutron-star mergers GW170817 and GW190425 by matching the observed GW data with theoretical GW models that depend on neutron-star properties.
5. Kilonova AT2017gfo associated with the GW signal. Kilonovae originate from the radioactive decay of heavy atomic nuclei created in nucleosynthesis processes during and after the merger of neutron stars, and are visible in the optical, infrared, and ultraviolet spectra. The EM observations are analysed with full radiative transfer simulations to extract information from the observed light curve and spectra.



# Multi-messenger astrophysics information

1. Mass measurements of the massive neutron stars PSR J0348+4042 and PSR J1614-2230  
→ lower bound on the NS maximum mass

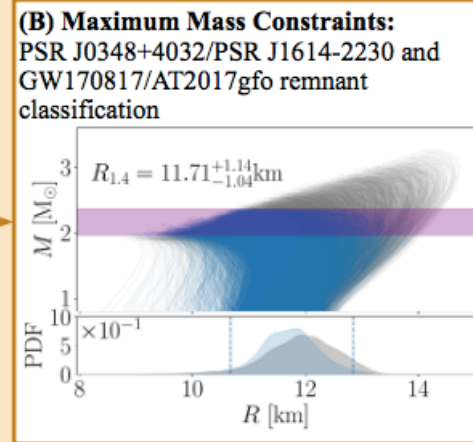
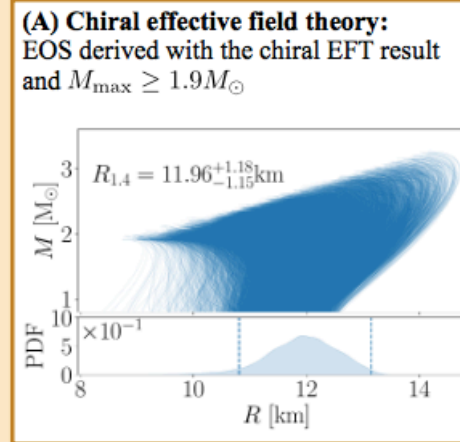
2. Binary neutron-star collision GW170817  
in which a black hole was presumably formed after the coalescence maximum mass of neutron stars  
→ upper bound on the maximum mass.

3. X-ray pulse-profile modelling of PSR J0030+0451 and PSR J0740+6620 using data from NICER and the X-ray Multi-Mirror Mission (XMM-Newton) are incorporated.
4. Bayesian inference techniques to analyse GW information from the 2 neutron-star mergers GW170817 and GW190425 by matching the observed GW data with theoretical GW models that depend on neutron-star properties.
5. Kilonova AT2017gfo associated with the GW signal. Kilonovae originate from the radioactive decay of heavy atomic nuclei created in nucleosynthesis processes during and after the merger of neutron stars, and are visible in the optical, infrared, and ultraviolet spectra. The EM observations are analysed with full radiative transfer simulations to extract information from the observed light curve and spectra.

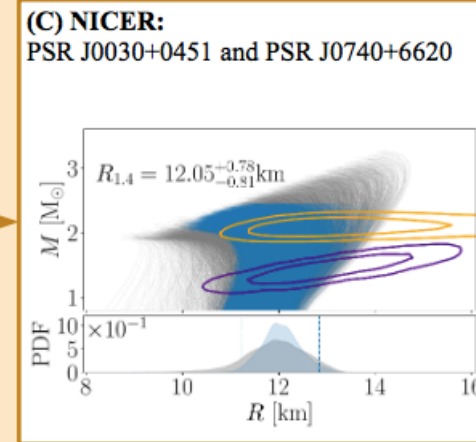


# Multi-messenger astrophysics information

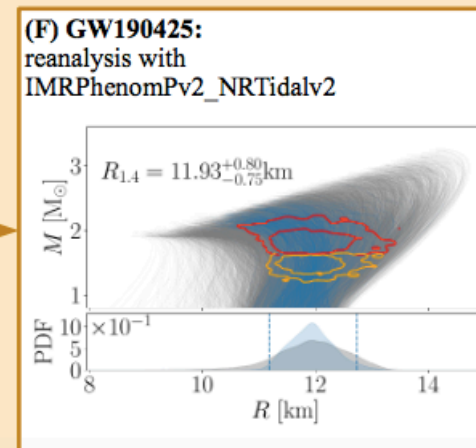
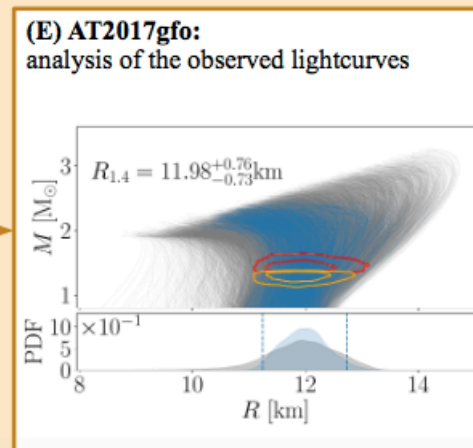
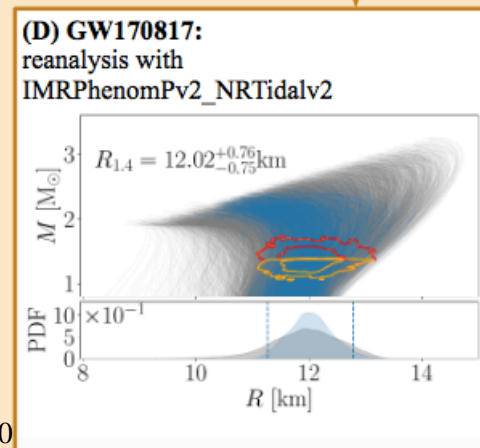
## Prior construction



Huth, Pang et al., arXiv:2107.06229



## Parameter estimation



Constraints are strongest above  $1.5\rho_0$ , where the extrapolation in the speed of sound is used for the EOSs. The high-density astrophysical constraints affect mostly the high-mass region in the mass-radius plane and exclude the stiffest EOSs that lead to the largest radii.

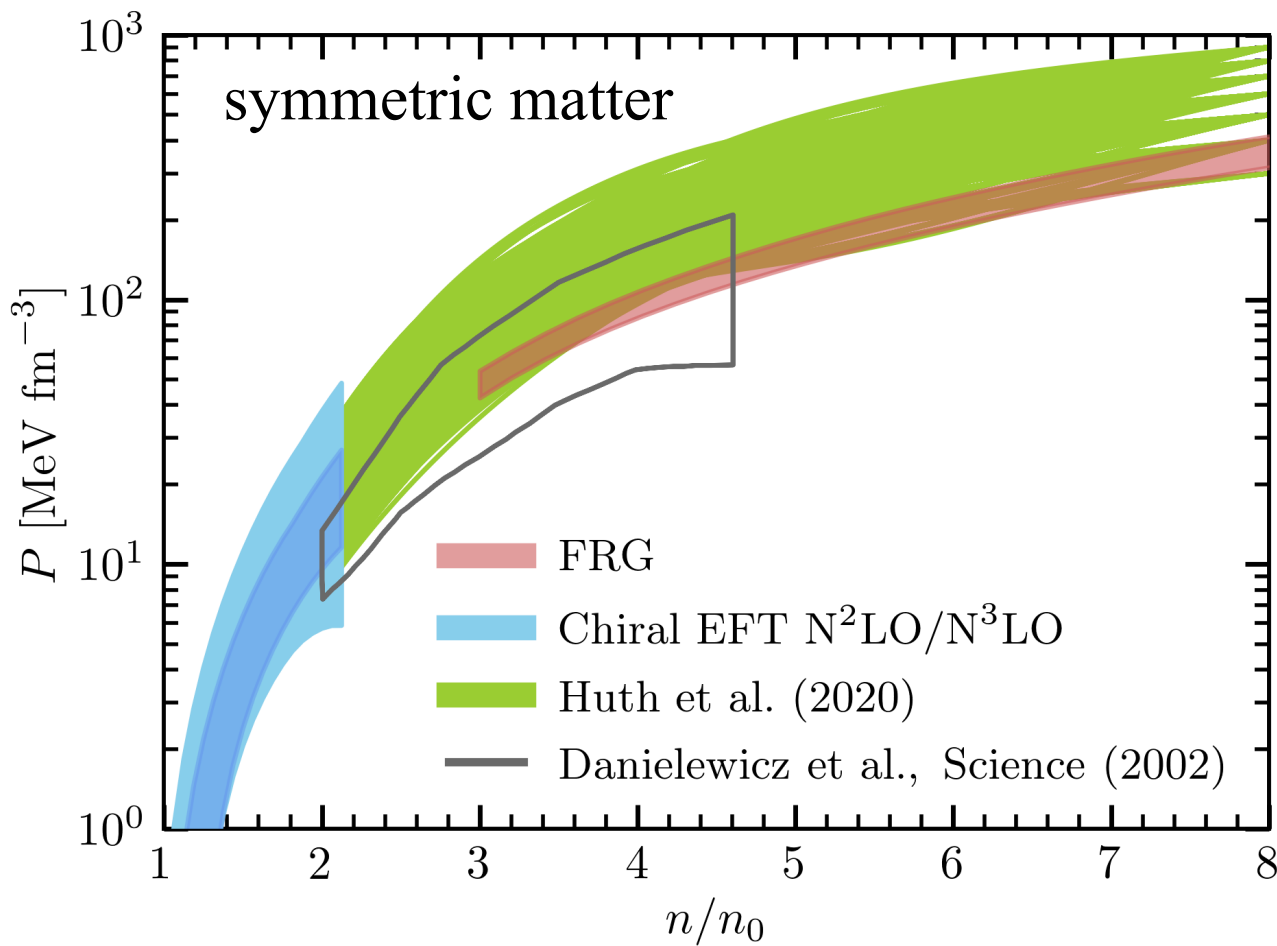
# Constraints from heavy-ion collisions

Comparison to **new EOS functionals** with  $2 M_{\odot}$  + LIGO/Virgo, NICER

Huth, Wellenhofer, AS (2021)

Comparison to pioneering  
heavy-ion constraint

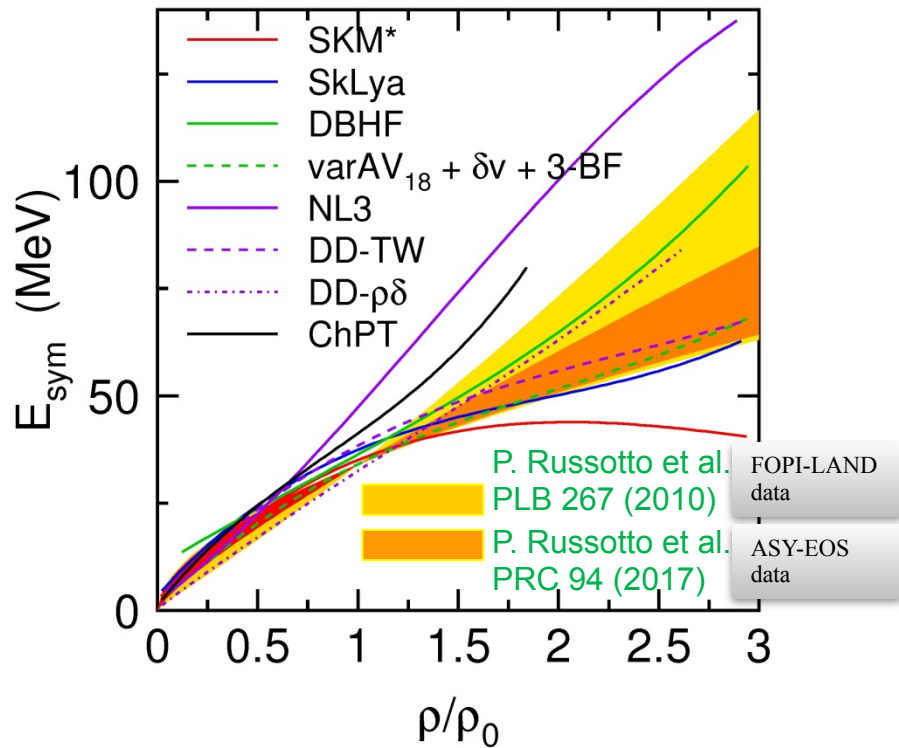
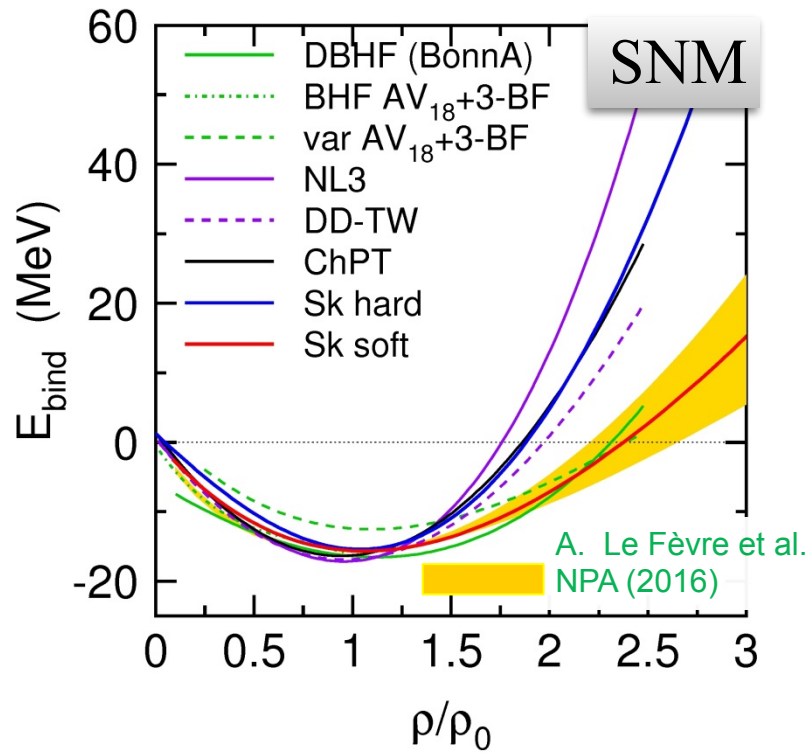
Danielewicz et al., Science (2002)



from Huth, Wellenhofer, AS, PRC (2021)

# Constraints from heavy-ion collisions

Synthesis at high densities of newest and most accurate HIC constraints



- equation of state of symmetric nuclear matter (SNM): FOPI (and KAOS)
- asymmetry energy: ASY-EOS
  - can be constrained by the systematic study of comparison of the flow of neutrons, protons and charged particles

# Constraints from heavy-ion collisions

How can we combine FOPI, ASY-EOS and ALADiN results  
to deduce **the pressure in a neutron star?**

- Have  $(P_{NN}^{sym}(K_0) + P_{asy}(L))\delta$   
 $\delta = 0.9(5\% \text{ protons} + \text{degenerate } e^-)$
- L as from ASY-EOS at  $1-2\rho_0$
- L as from ALADiN at  $0.7\rho_0$  (preliminary)
- $K_0$  as from FOPI flow data

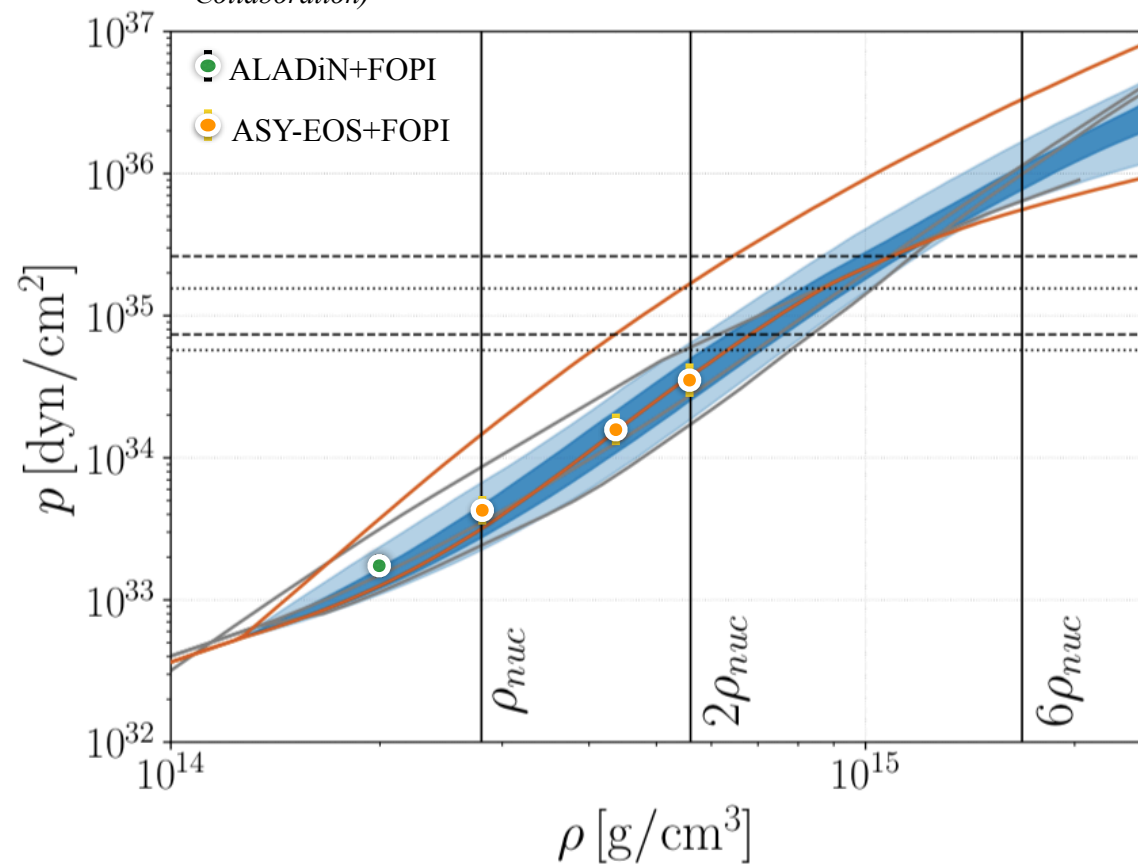
# Constraints from heavy-ion collisions

How can we combine FOPI, ASY-EOS and ALADiN results to deduce the pressure in a neutron star?

- Have  $(P_{NN}^{sym}(K_0) + P_{asy}(L))\delta$   
 $\delta = 0.9(5\% \text{ protons} + \text{degenerate } e^-)$
- L as from ASY-EOS at  $1-2\rho_0$
- L as from ALADiN at  $0.7\rho_0$  (preliminary)
- $K_0$  as from FOPI flow data

Gravitational Wave 170817

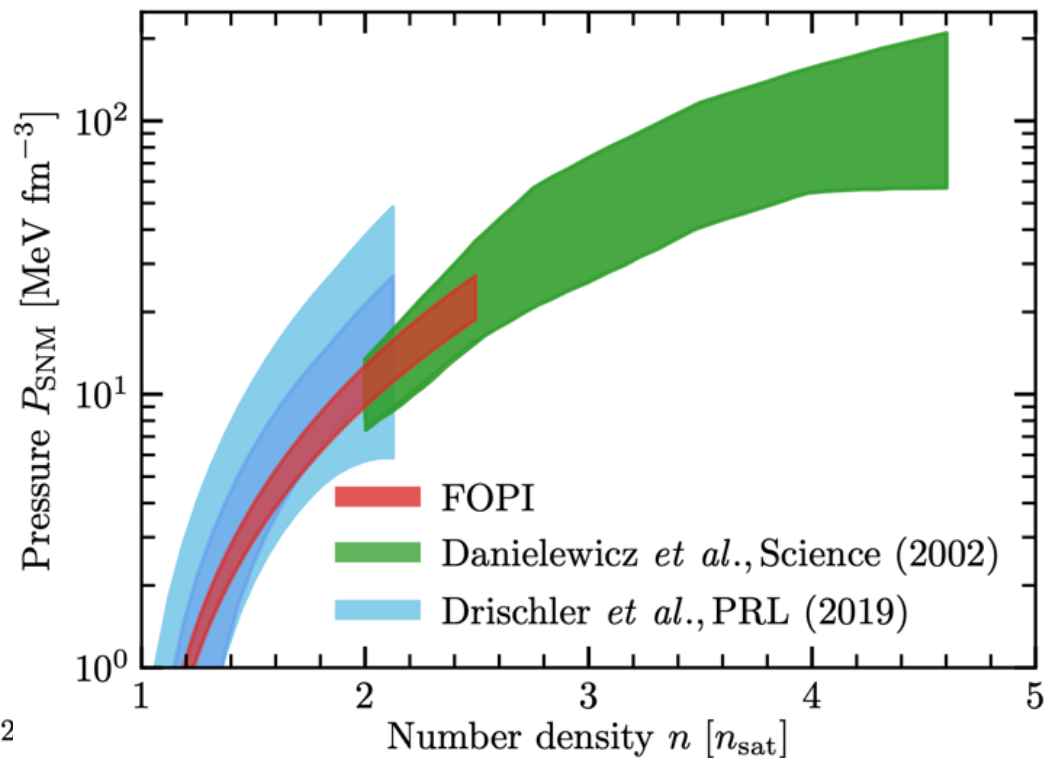
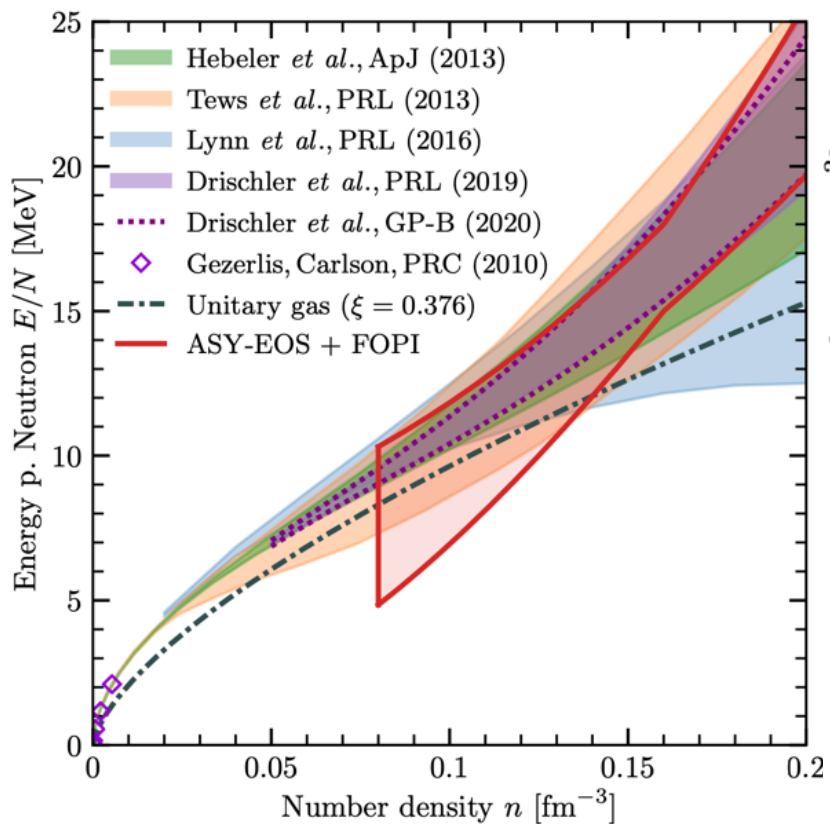
B. P. Abbott et al. (The LIGO Scientific Collaboration and the Virgo Collaboration)



# Constraints from heavy-ion collisions

Huth, Pang et al., arXiv:2107.06229

Include in addition to chiral EFT: constraints from ASY-EOS and FOPI for neutron and symmetric matter with different functionals



# Constraints from heavy-ion collisions

Huth, Pang et al., arXiv:2107.06229

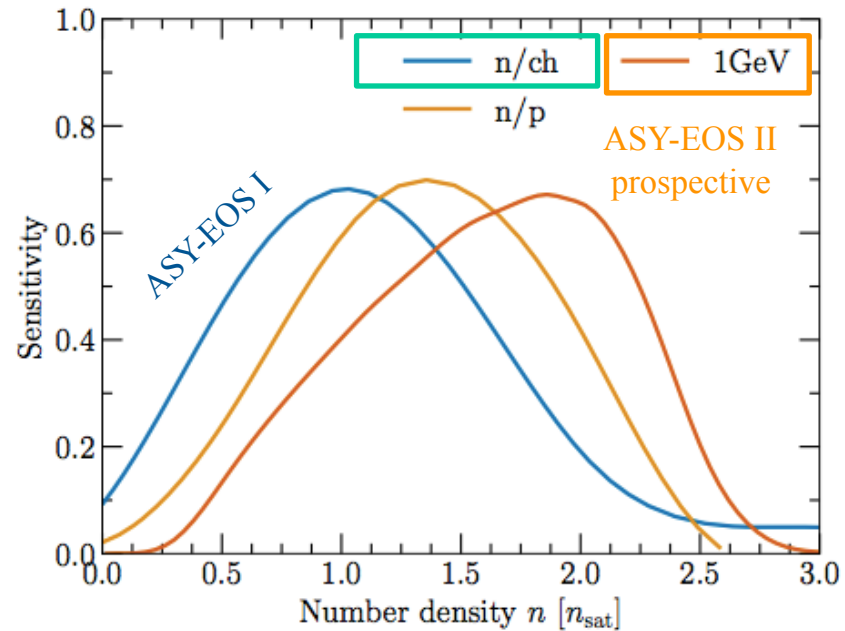
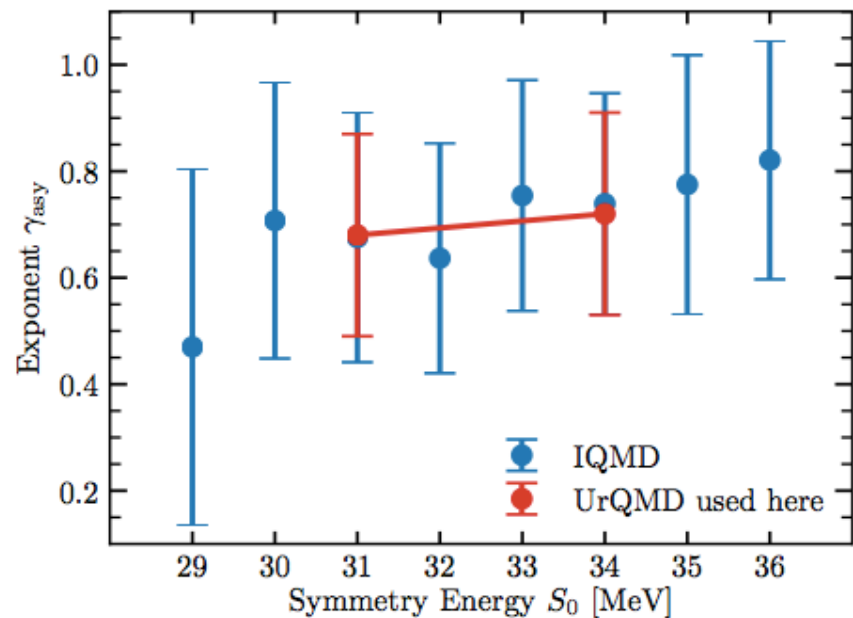
Introducing in the HIC prior a series of EoS samples according to intervals of variation of  $\gamma_{asy}$ ,  $S_0$ ,  $K_0$

with a weight following the density sensitivity curve constrained by ASY-EOS (more limited than that of FOPI+AGS)

$$E_{asy} = E_{asy}^{pot} + E_{asy}^{kin} = E_0^{pot} \left(\frac{\rho}{\rho_0}\right)^\gamma + E_0^{kin} \left(\frac{\rho}{\rho_0}\right)^{2/3}$$

$$S_0 = E_0^{pot} + E_0^{kin}$$

ASY-EOS data constraint (Au+Au @ 400A MeV)



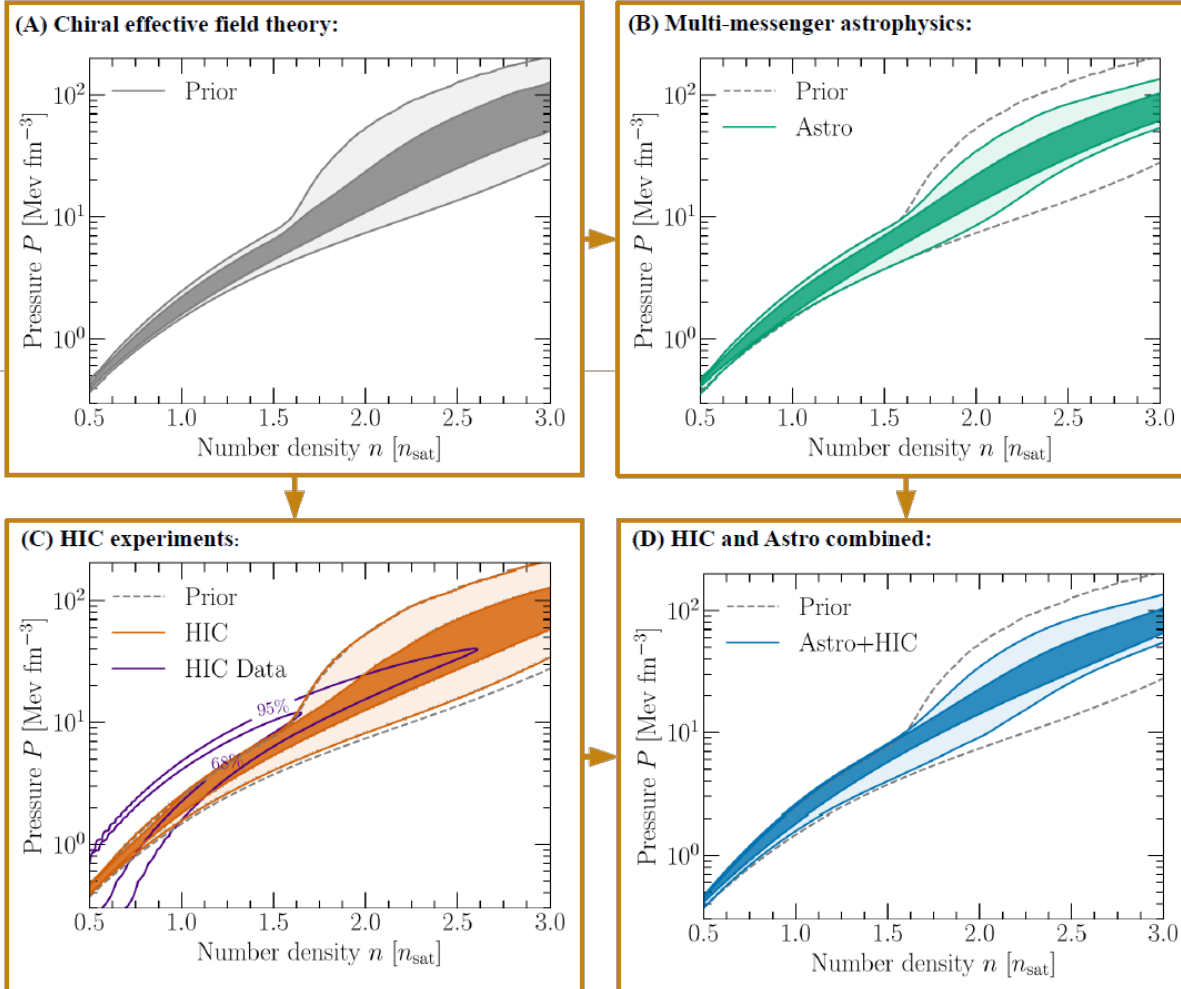
→ Linear relation between  $\gamma_{asy}$  and  $S_0$

# Constraints from heavy-ion collisions

Combining astronomical multimessengers and HIC's within the same bayesian analysis to constrain the neutron star matter EoS:

Huth, Pang et al., arXiv:2107.06229

« **HIC** » = FOPI+ASY-EOS+AGS - « **Astro** » = GW, NICER (pulsar X-ray hot spots)

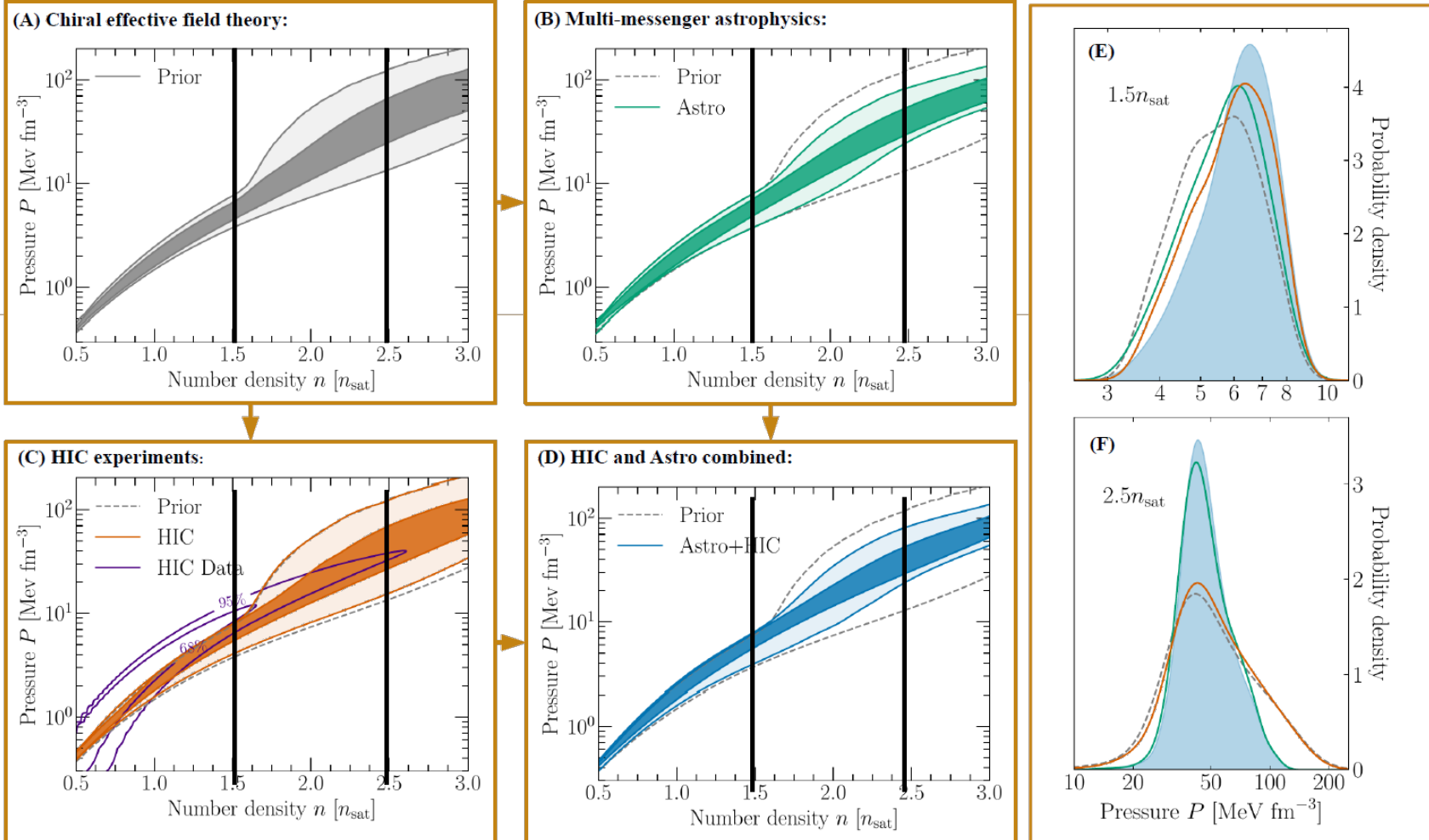


# Constraints from heavy-ion collisions

Combining astronomical multimessengers and HIC's within the same bayesian analysis to constrain the neutron star matter EoS:

Huth, Pang et al., arXiv:2107.06229

« HIC » = FOPI+ASY-EOS+AGS - « Astro » = GW, NICER (pulsar X-ray hot spots)

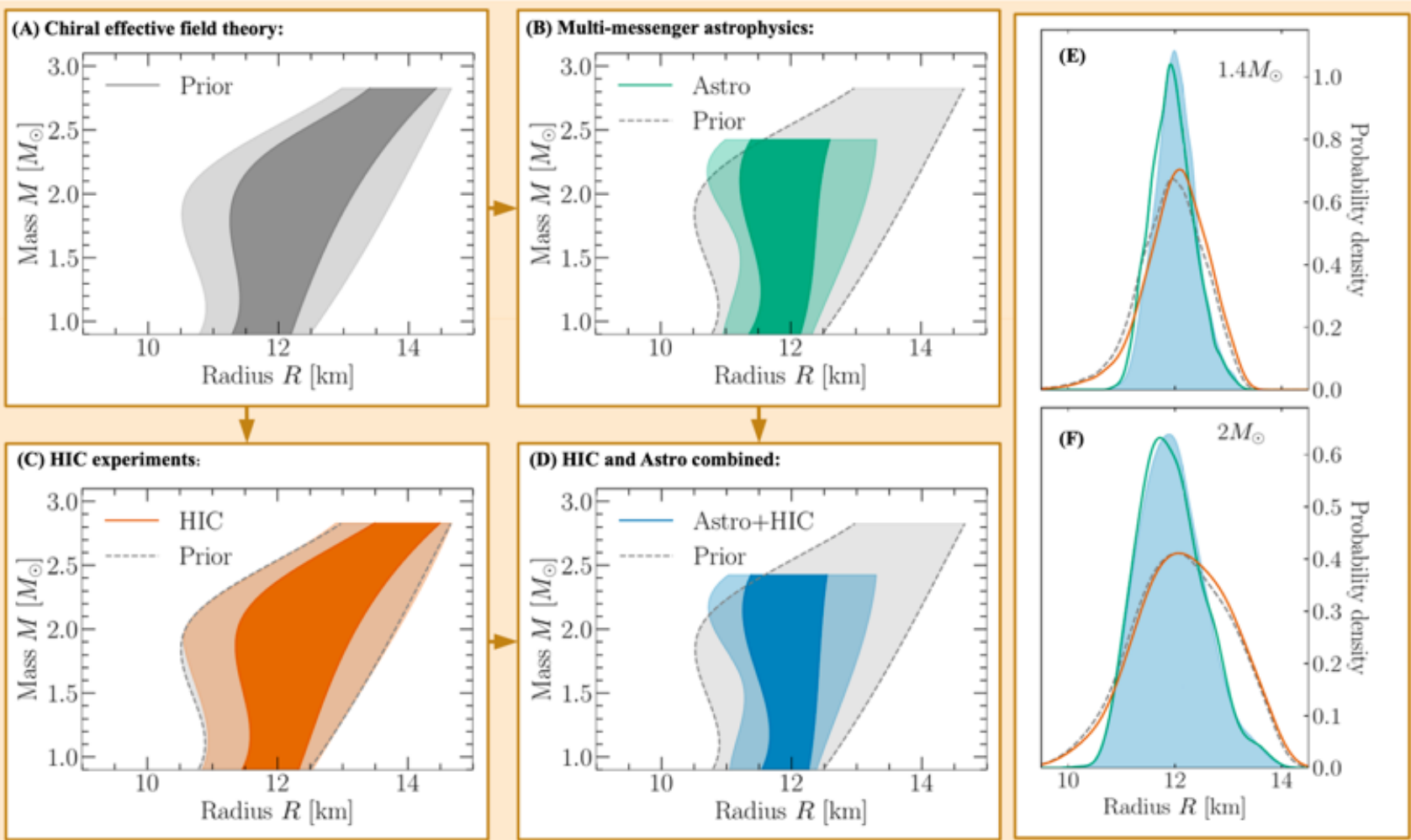


# Constraints from heavy-ion collisions

Combining astronomical multimessengers and HIC's within the same bayesian analysis to constrain the neutron star matter EoS:

Huth, Pang et al., arXiv:2107.06229

« HIC » = FOPI+ASY-EOS+AGS - « Astro » = GW, NICER (pulsar X-ray hot spots)



# Constraints from heavy-ion collisions

Combining astronomical multimessengers and HIC's within the same bayesian analysis to constrain the neutron star matter EoS:

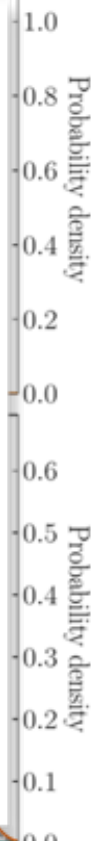
Huth, Pang et al., arXiv:2107.06229

« **HIC** » = FOPI+ASY-EOS+AGS - « **Astro** » = GW, NICER (pulsar X-ray hot spots)

(A) Chiral effective field theory:

(B) Multi-messenger astrophysics:

- HIC constraints prefer higher pressures, similar to NICER, **overall remarkable consistency** with chiral EFT and astro constraints!
- **Up to  $1.5\rho_0$** , HIC's constrain the neutron star EoS with a **similar accuracy** as Astro most recent findings, favouring a somehow **stiffer EoS (higher pressure)**.
- **Above  $1.5\rho_0$** , Astro measurements are **still more accurate**, and drive the NS EoS, though with lower statistics.
- Most significant densities for constraining NS radii:
  - for  $1.4M_\odot$  :  $\rho \approx 1.6\rho_0$
  - for  $2M_\odot$  :  $\rho \approx 2 - 2.5\rho_0$
- HIC's can enhance its contribution at larger densities by 2 ways : probe higher densities (higher incident energies), improve the accuracy of E<sub>asy</sub> constraint.

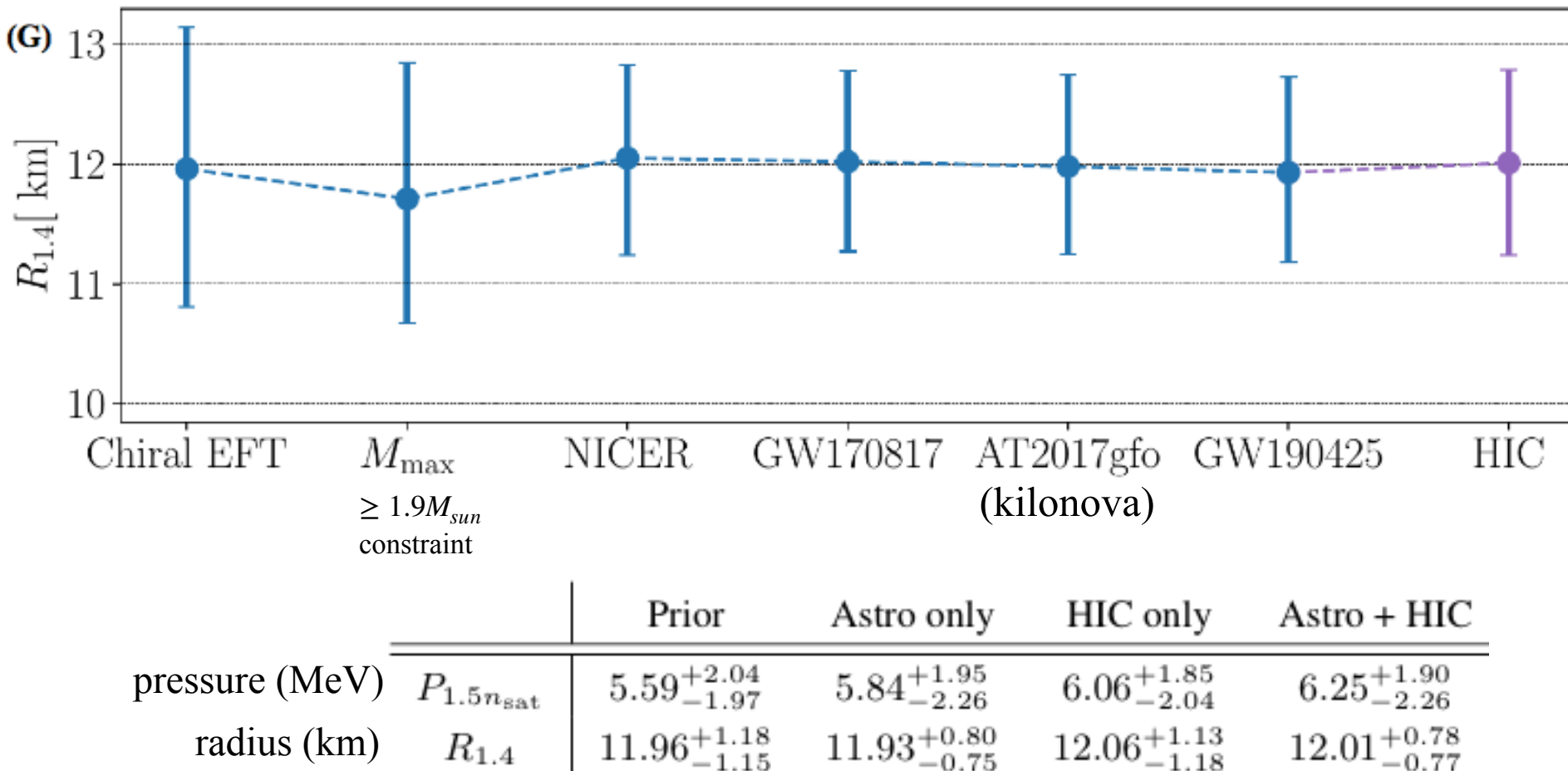


# Constraints from heavy-ion collisions

Huth, Pang et al., arXiv:2107.06229

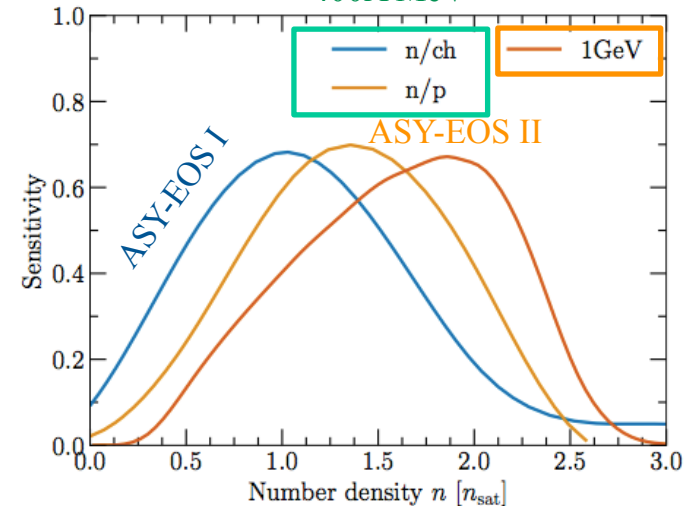
- Inclusion of HIC constraints prefers higher pressures, similar to NICER.
- Overall remarkable consistency with HIC and astro constraints!

« **HIC** » = FOPI+ASY-EOS+AGS - « **Astro** » = GW, NICER (pulsar X-ray hot spots)



# Perspectives

Huth, Pang et al., arXiv:2107.06229  
400A MeV



## ASY-EOS II @ GSI

- **larger densities probed:**  
higher incident energies: Au+Au @ 250 - 1000 MeV/nucleon
- **improved accuracy** on  $E_{asy}$  constraint:  
with n, p, d, t identification in NeuLAND with large efficiency

Predictions with present Easy HIC constraint:

ASY-EOS I @ 400A MeV    ASY-EOS II @ 400A MeV    ASY-EOS II @ 1A GeV

P/R	Current setup			1GeV sensitivity		1GeV sensitivity and halved uncertainty on HIC		1GeV sensitivity with a 1 $n_{sat}$ lower cutoff	
	HIC only	Astro	Astro+HIC	HIC only	Astro+HIC	HIC only	Astro+HIC	HIC only	Astro+HIC
pressure (MeV)	1.0 $n_{sat}$	2.05 <sup>+0.49</sup> <sub>-0.45</sub>	2.00 <sup>+0.52</sup> <sub>-0.49</sub>	2.11 <sup>+0.49</sup> <sub>-0.52</sub>	2.10 <sup>+0.49</sup> <sub>-0.45</sub>	2.13 <sup>+0.47</sup> <sub>-0.53</sub>	2.12 <sup>+0.43</sup> <sub>-0.48</sub>	2.16 <sup>+0.43</sup> <sub>-0.55</sub>	2.07 <sup>+0.48</sup> <sub>-0.45</sub>
	1.5 $n_{sat}$	6.06 <sup>+1.85</sup> <sub>-2.04</sub>	5.84 <sup>+1.96</sup> <sub>-2.26</sub>	6.25 <sup>+1.90</sup> <sub>-2.26</sub>	6.20 <sup>+1.71</sup> <sub>-2.13</sub>	6.35 <sup>+1.80</sup> <sub>-2.31</sub>	5.84 <sup>+1.96</sup> <sub>-2.26</sub>	6.44 <sup>+1.77</sup> <sub>-2.21</sub>	6.11 <sup>+1.80</sup> <sub>-2.02</sub>
	2.0 $n_{sat}$	19.47 <sup>+33.63</sup> <sub>-11.67</sub>	18.44 <sup>+16.24</sup> <sub>-9.69</sub>	19.07 <sup>+15.27</sup> <sub>-10.53</sub>	19.42 <sup>+28.90</sup> <sub>-11.69</sub>	19.14 <sup>+14.24</sup> <sub>-8.97</sub>	19.73 <sup>+29.32</sup> <sub>-11.49</sub>	19.32 <sup>+13.93</sup> <sub>-8.74</sub>	18.66 <sup>+22.18</sup> <sub>-8.65</sub>
	2.5 $n_{sat}$	47.78 <sup>+75.96</sup> <sub>-32.96</sub>	45.05 <sup>+39.80</sup> <sub>-19.62</sub>	45.43 <sup>+40.41</sup> <sub>-19.11</sub>	47.13 <sup>+75.65</sup> <sub>-27.86</sub>	45.3 <sup>+40.52</sup> <sub>-17.24</sub>	48.20 <sup>+78.30</sup> <sub>-24.83</sub>	45.73 <sup>+38.03</sup> <sub>-18.47</sub>	44.31 <sup>+60.85</sup> <sub>-21.23</sub>
radius (km)	1.0 $M_{\odot}$	11.89 <sup>+0.79</sup> <sub>-0.98</sub>	11.76 <sup>+0.65</sup> <sub>-0.71</sub>	11.88 <sup>+0.57</sup> <sub>-0.76</sub>	11.91 <sup>+0.74</sup> <sub>-0.93</sub>	11.91 <sup>+0.55</sup> <sub>-0.76</sub>	11.96 <sup>+0.72</sup> <sub>-0.85</sub>	11.94 <sup>+0.54</sup> <sub>-0.71</sub>	11.85 <sup>+0.66</sup> <sub>-0.78</sub>
	1.4 $M_{\odot}$	12.06 <sup>+1.13</sup> <sub>-1.18</sub>	11.94 <sup>+0.79</sup> <sub>-0.78</sub>	12.01 <sup>+0.78</sup> <sub>-0.77</sub>	12.08 <sup>+1.09</sup> <sub>-1.10</sub>	12.02 <sup>+0.76</sup> <sub>-0.73</sub>	12.11 <sup>+1.07</sup> <sub>-1.01</sub>	12.04 <sup>+0.72</sup> <sub>-0.71</sub>	11.97 <sup>+0.95</sup> <sub>-0.85</sub>
	1.6 $M_{\odot}$	12.11 <sup>+1.33</sup> <sub>-1.33</sub>	11.98 <sup>+0.93</sup> <sub>-0.79</sub>	12.03 <sup>+0.98</sup> <sub>-0.75</sub>	12.12 <sup>+1.30</sup> <sub>-1.24</sub>	12.04 <sup>+0.88</sup> <sub>-0.75</sub>	12.15 <sup>+1.26</sup> <sub>-1.16</sub>	12.06 <sup>+0.85</sup> <sub>-0.74</sub>	11.99 <sup>+1.14</sup> <sub>-0.95</sub>
	2.0 $M_{\odot}$	12.19 <sup>+1.71</sup> <sub>-1.59</sub>	11.88 <sup>+1.23</sup> <sub>-1.10</sub>	11.91 <sup>+1.24</sup> <sub>-1.11</sub>	12.17 <sup>+1.71</sup> <sub>-1.51</sub>	11.90 <sup>+1.21</sup> <sub>-1.10</sub>	12.18 <sup>+1.66</sup> <sub>-1.46</sub>	11.92 <sup>+1.19</sup> <sub>-1.07</sub>	11.93 <sup>+1.61</sup> <sub>-1.32</sub>

# Perspectives

Astro-multimessenger  
future program



# Conclusion and perspectives



# Conclusion and perspectives

- Combining FOPI, ASY-EOS (and AGS) results allows to predict a density dependance of the pressure in a neutron star, from  $\approx 0.5\rho_0$  to  $\approx 2\rho_0$ , with a challenging accuracy (though improvable), remarkably in agreement with recent astrophysical measurements deduced from multimessengers and chiral EFT. A future AsyEOS experiment is planned at GSI at higher incident energy to further constrain the asymmetry energy up to  $\approx 3\rho_0$ .



# Conclusion and perspectives

- Combining FOPI, ASY-EOS (and AGS) results allows to predict a density dependance of the pressure in a neutron star, from  $\approx 0.5\rho_0$  to  $\approx 2\rho_0$ , with a challenging accuracy (though improvable), remarkably in agreement with recent astrophysical measurements deduced from multimessengers and chiral EFT. A future AsyEOS experiment is planned at GSI at higher incident energy to further constrain the asymmetry energy up to  $\approx 3\rho_0$ .
- Perspective: improve HIC input at sub-saturation densities with accurate  $E_{asy}$  constraints.



# Conclusion and perspectives

- Combining FOPI, ASY-EOS (and AGS) results allows to predict a density dependance of the pressure in a neutron star, from  $\approx 0.5\rho_0$  to  $\approx 2\rho_0$ , with a challenging accuracy (though improvable), remarkably in agreement with recent astrophysical measurements deduced from multimessengers and chiral EFT. A future AsyEOS experiment is planned at GSI at higher incident energy to further constrain the asymmetry energy up to  $\approx 3\rho_0$ .
- Perspective: improve HIC input at sub-saturation densities with accurate  $E_{asy}$  constraints.
- Promising combination of HIC constraints with effective field theory of strong interaction + powerful many-body theory.



# Conclusion and perspectives

- Combining FOPI, ASY-EOS (and AGS) results allows to predict a density dependance of the pressure in a neutron star, from  $\approx 0.5\rho_0$  to  $\approx 2\rho_0$ , with a challenging accuracy (though improvable), remarkably in agreement with recent astrophysical measurements deduced from multimessengers and chiral EFT. A future AsyEOS experiment is planned at GSI at higher incident energy to further constrain the asymmetry energy up to  $\approx 3\rho_0$ .
- Perspective: improve HIC input at sub-saturation densities with accurate  $E_{asy}$  constraints.
- Promising combination of HIC constraints with effective field theory of strong interaction + powerful many-body theory.
- Beyond  $3 - 4\rho_0$  (FAIR, NICA), new observables needed to constrain SNM and NS EoS. A new generation of relativistic transport models must arise, benchmarked e.g. with data taken at SIS18 at the highest available beam energies (FOPI, HADES).

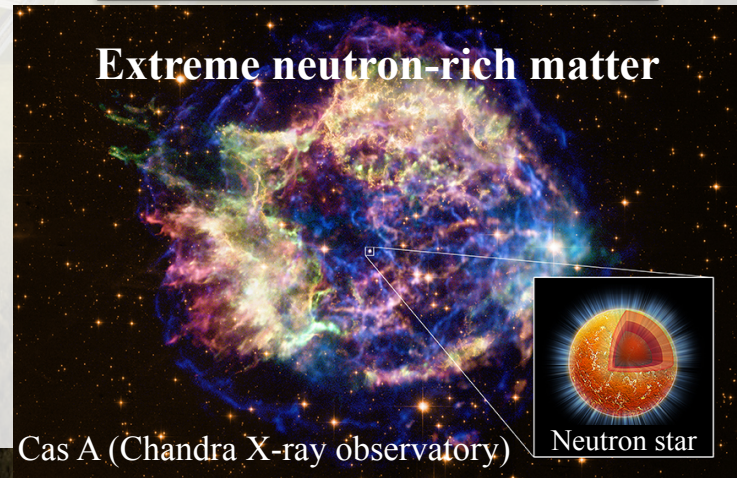
# Conclusion and perspectives

- Combining FOPI, ASY-EOS (and AGS) results allows to predict a density dependance of the pressure in a neutron star, from  $\approx 0.5\rho_0$  to  $\approx 2\rho_0$ , with a challenging accuracy (though improvable), remarkably in agreement with recent astrophysical measurements deduced from multimessengers and chiral EFT. A future AsyEOS experiment is planned at GSI at higher incident energy to further constrain the asymmetry energy up to  $\approx 3\rho_0$ .
- Perspective: improve HIC input at sub-saturation densities with accurate  $E_{asy}$  constraints.
- Promising combination of HIC constraints with effective field theory of strong interaction + powerful many-body theory.
- Beyond  $3 - 4\rho_0$  (FAIR, NICA), new observables needed to constrain SNM and NS EoS. A new generation of relativistic transport models must arise, benchmarked e.g. with data taken at SIS18 at the highest available beam energies (FOPI, HADES).

New experimental frontier

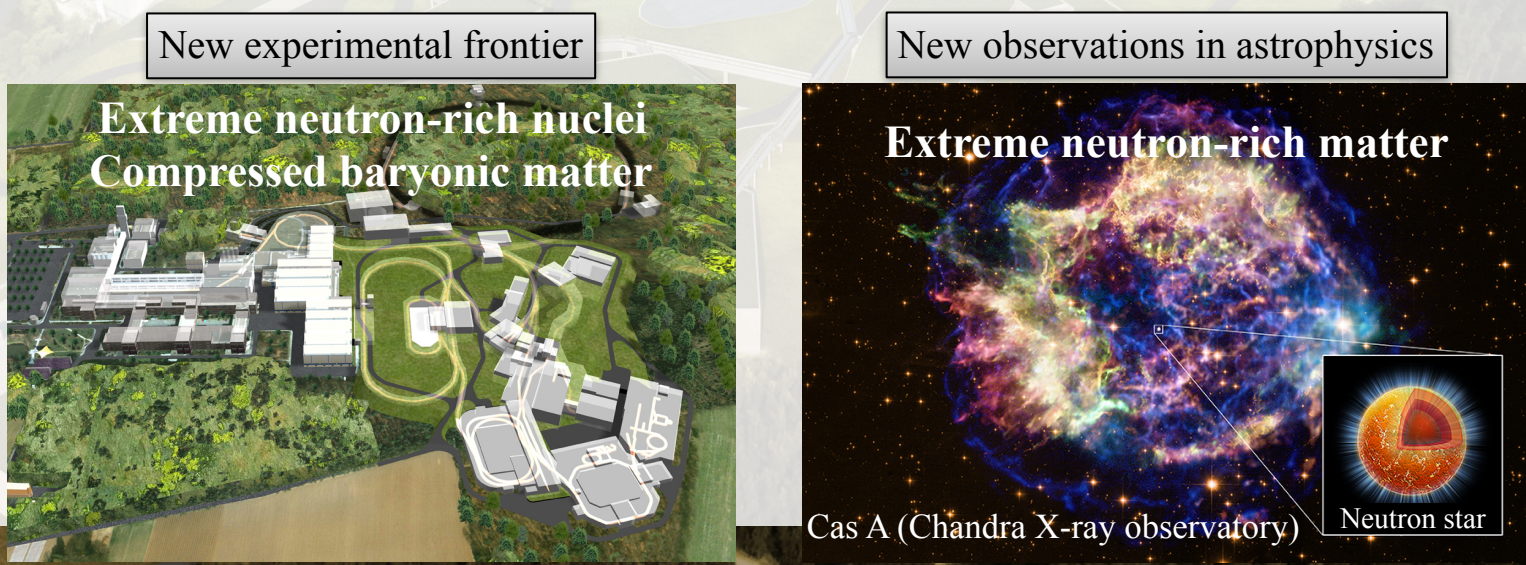


New observations in astrophysics



# Conclusion and perspectives

- Combining FOPI, ASY-EOS (and AGS) results allows to predict a density dependance of the pressure in a neutron star, from  $\approx 0.5\rho_0$  to  $\approx 2\rho_0$ , with a challenging accuracy (though improvable), remarkably in agreement with recent astrophysical measurements deduced from multimessengers and chiral EFT. A future AsyEOS experiment is planned at GSI at higher incident energy to further constrain the asymmetry energy up to  $\approx 3\rho_0$ .
- Perspective: improve HIC input at sub-saturation densities with accurate  $E_{asy}$  constraints.
- Promising combination of HIC constraints with effective field theory of strong interaction + powerful many-body theory.
- Beyond  $3 - 4\rho_0$  (FAIR, NICA), new observables needed to constrain SNM and NS EoS. A new generation of relativistic transport models must arise, benchmarked e.g. with data taken at SIS18 at the highest available beam energies (FOPI, HADES).



Thanks to collaborators:

especially Sabrina Huth, Peter T. H. Pang, Ingo Tews, Tim Dietrich, Achim Schwenk, Wolfgang Trautmann, Kshitij Agarwal, Mattia Bulla, Michael W. Coughlin, Chris Van Den Broeck, and P. Russotto, D. Cozma, Ch. Hartnack.